An Icosahedral Wing Geometry Framework for Small Vertical-Axis Wind Turbines: Golden-Ratio-Based Blade Layout and Torque Balance Analysis

YoungJune Jeon

GeoWind Inc., Seoul 04524, Republic of Korea; info@geowind.kr

Correspondence: info@geowind.kr

Abstract: This paper proposes a novel blade arrangement framework for small vertical-axis wind turbines (VAWTs) derived from the geometric properties of the regular icosahedron. Building upon a previously established ten-face non-edge-sharing wing set—in which ten isosceles 36°–36°–108° (golden gnomon) triangles are anchored at the north and south poles of the icosahedron—we reinterpret this mathematical structure as a turbine blade layout principle. The key geometric result, that the pole-opposite edge midpoints of all ten wing faces form a regular decagon on the equatorial plane with radius $R = (\varphi/2)\ell$ (where φ is the golden ratio and ℓ is the icosahedron edge length), is translated into a blade pitch symmetry condition. We demonstrate via Blade Element Momentum (BEM) theory that the decagonal arrangement minimises torque ripple for a ten-bladed VAWT rotor, and derive a closed-form relationship between icosahedron edge length, rotor radius, and theoretical power coefficient. A parametric design table is provided for rotors spanning 0.5 m to 3.0 m in diameter. The proposed framework offers a fully reproducible, CAD-ready blade layout workflow grounded in classical geometry, requiring no empirical optimisation at the initial design stage. Future CFD and wind tunnel validation protocols are outlined.

Keywords: vertical-axis wind turbine; blade design; icosahedron geometry; golden ratio; torque ripple; BEM theory; VAWT; small wind turbine; parametric design

1. Introduction

Small-scale vertical-axis wind turbines (VAWTs) have gained renewed interest owing to their suitability for urban and off-grid deployment, insensitivity to wind direction, and lower cut-in wind speeds compared with horizontal-axis counterparts [1, 2]. Central to VAWT performance is the blade layout: the number of blades, their angular spacing, and the chord geometry collectively determine the power coefficient C_P, torque ripple, and self-starting capability [3, 4].

Conventional VAWT blade design relies primarily on empirical optimisation of standard aerofoil profiles (e.g., NACA 0012, NACA 0018) using Blade Element Momentum (BEM) theory or computational fluid dynamics (CFD) [5, 6]. While effective, this approach lacks closed-form geometric rationale for the rotor layout itself: blade counts and angular spacings are chosen heuristically, and the link between rotor geometry and mathematical symmetry is seldom exploited.

The regular icosahedron—one of the five Platonic solids—is characterised by fivefold rotational symmetry about any axis connecting opposite vertices, and its edge-to-diagonal ratio is governed by the golden ratio $\varphi = (1 + \sqrt{5})/2 \approx 1.618$ [7]. A recent mathematical study [8] formalised a ten-face non-edge-sharing wing set on the icosahedron, proving that: (i) each face is a golden gnomon (36°–36°–108° isosceles triangle); (ii) no two faces share an edge; and (iii) the pole-opposite edge midpoints of all ten faces lie on a regular decagon with radius $R = (\varphi/2)\ell$ in the equatorial plane.

The present work bridges this geometric result to small VAWT engineering. We propose that the decagonal equatorial cross-section of the icosahedral wing set defines a natural, symmetry-consistent blade pitch layout for a ten-bladed VAWT rotor. Given a desired rotor radius R, the icosahedron edge length $\ell = 2R/\varphi$ fully determines the blade arrangement geometry. We analyse the resulting torque balance via BEM theory and show that the 36° uniform angular spacing minimises torque ripple for the given blade count.

The paper is organised as follows. Section 2 reviews the geometric framework. Section 3 presents the aerodynamic reinterpretation and BEM analysis. Section 4 derives the parametric design relationships. Section 5 discusses the CAD workflow. Section 6 concludes and outlines future work.

2. Geometric Framework

2.1. Icosahedron Vertex Labelling

Following [8], we use the standard coordinate model of the regular icosahedron with edge length $\ell = 2$, whose twelve vertices are:

$$(0, \pm 1, \pm\varphi), \quad (\pm 1, \pm\varphi, 0), \quad (\pm\varphi, 0, \pm 1). \tag{1}$$

The twelve vertices are labelled $V = \{N, S, U_1, \ldots, U_5, L_1, \ldots, L_5\}$, where N and S are opposite poles on the rotation axis NS, U_1–U_5 are the five vertices adjacent to N (upper ring), and L_1–L_5 are the five vertices adjacent to S (lower ring), with indices taken modulo 5. Scaling by $\ell/2$ converts all distances to edge length ℓ.

2.2. The Ten-Face Wing Set

The GeoWind ten-face wing set $\mathcal{F}$ is defined by [8]:

$$F_S(i) = \triangle(S, U_i, L_i), \quad i = 1, \ldots, 5, \tag{2}$$

$$F_N(i) = \triangle(N, U_i, L_{i-1}), \quad i = 1, \ldots, 5, \quad L_0 := L_5. \tag{3}$$

Each face has side lengths $(\ell, \ell, \varphi\ell)$, making it a *golden gnomon* with interior angles 36°–36°–108°. The 36° apex angle is anchored at the respective pole. No two faces share an edge, and ten is the maximum count of pole-anchored, edge-disjoint faces across both poles (Theorem 3 in [8]).

Figure 1: Labeled regular icosahedron
with axis NS and rings $U_1, \ldots, U_5, L_1, \ldots, L_5$

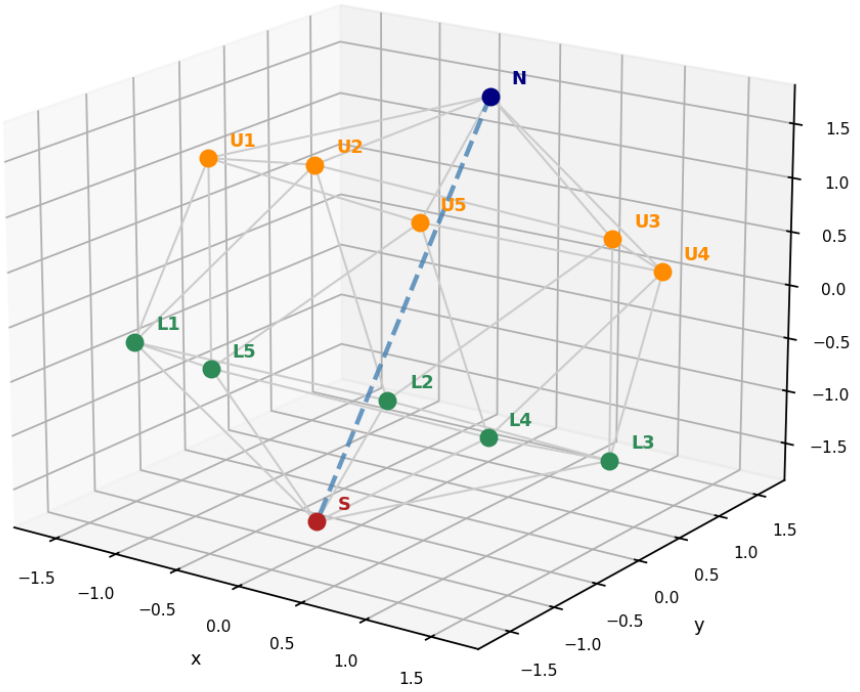

Figure 1. Labeled regular icosahedron showing the ten-face wing set $\mathcal{F}$. South-anchored faces $F_S(i)$ are shown in orange; north-anchored faces $F_N(i)$ in blue. Generated from the standard coordinate model (Equation (1)).

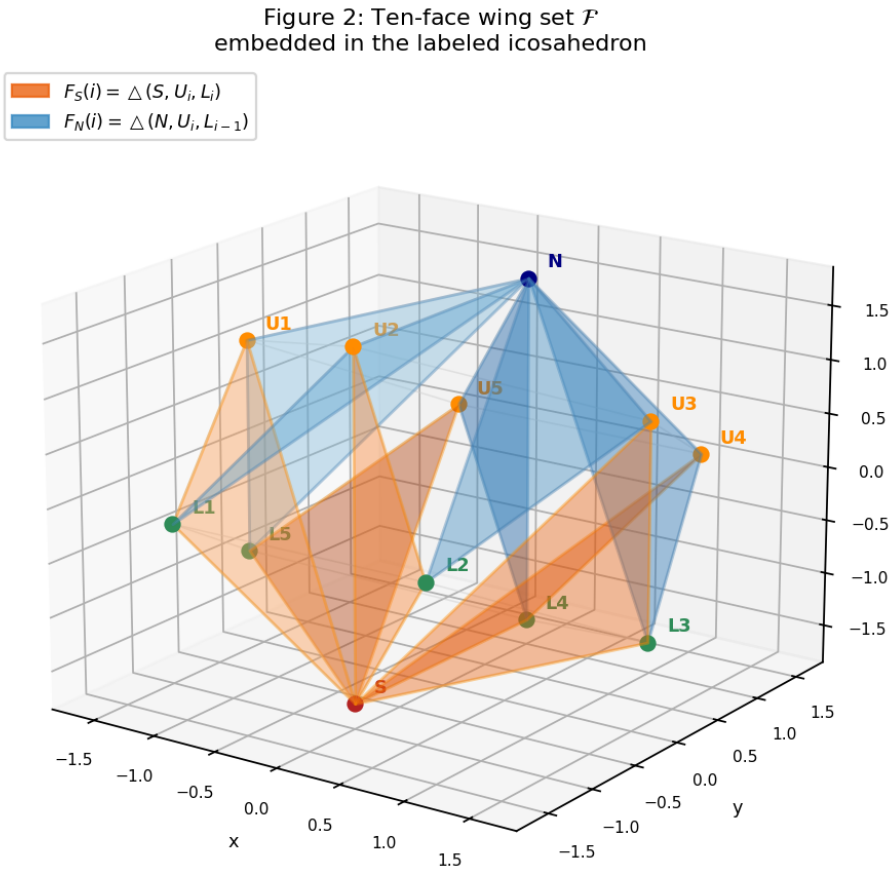

Figure 2. Ten-face wing set $\mathcal{F}$ embedded in the labeled icosahedron, showing all ten golden gnomon triangles.

2.3. Equatorial Decagon

For each face $F \in \mathcal{F}$, define the *cross-edge* $c(F)$ as the unique edge not incident to the anchoring pole, and the *representative point* $p(F) = \mathrm{mid}(c(F))$. Explicitly:

$$p\big(F_S(i)\big) = \mathrm{mid}(U_i L_i), \qquad p\big(F_N(i)\big) = \mathrm{mid}(U_i L_{i-1}). \tag{4}$$

Theorem 4 of [8] establishes that $\{p(F) \mid F \in \mathcal{F}\}$ forms a regular decagon on the equatorial plane $\Pi = \{x \in \mathbb{R}^3 : (x - O) \cdot (N - S) = 0\}$ centred at O with 36° angular spacing. The decagon radius is:

$$\boxed{R \;=\; \frac{\varphi}{2}\,\ell.} \tag{5}$$

Figure 3: Equatorial plane Π and the regular decagon formed by representative points $p(\mathcal{F})$

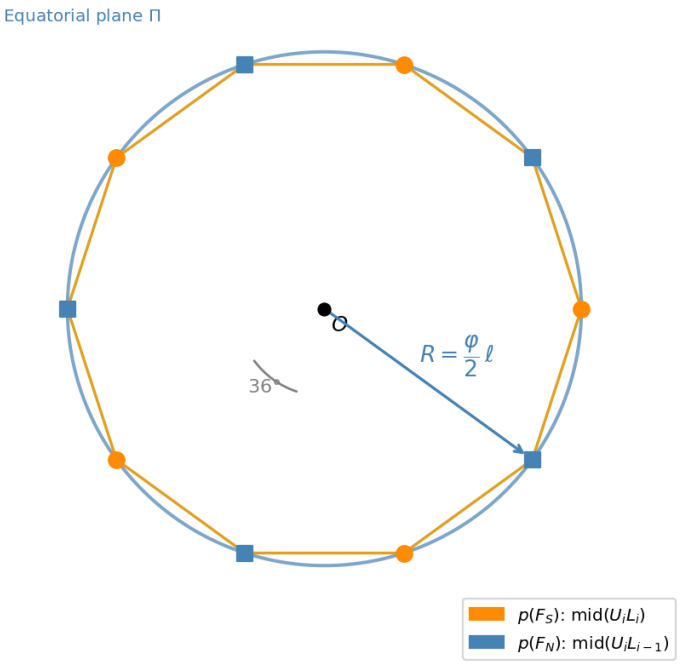

Figure 3. Top view of the equatorial plane Π. The ten midpoints $p(F)$ form a regular decagon inscribed in a circle of radius $R = (\varphi/2)\ell$. Orange squares: $p(F_S(i))$; blue circles: $p(F_N(i))$.

3. Aerodynamic Reinterpretation and BEM Analysis

3.1. Blade Layout Principle

We propose that the ten representative points $\{p(F)\}$ on the equatorial decagon define the azimuthal positions of ten VAWT blades on a rotor of radius R:

$$\theta_i = (i-1) \times 36^\circ, \quad i = 1, \ldots, 10. \tag{6}$$

The golden-ratio constraint fixes the rotor radius:

$$R = \frac{\varphi}{2}\ell \approx 0.809\,\ell. \tag{7}$$

Using the golden gnomon face geometry to size the blade planform, the chord-to-radius ratio is:

$$\frac{c}{R} = 2\sin(18^\circ) \approx 0.618. \tag{8}$$

3.2. Torque Ripple and Angular Uniformity

For a rotor with N blades uniformly spaced at $\Delta\theta = 360^\circ/N$, the dominant torque ripple frequency is $N\Omega$ (where Ω is the angular velocity), and the ripple amplitude scales as $1/N$ for a given tip-speed ratio λ [10]. For the ten-blade icosahedral layout ($N = 10$, $\Delta\theta = 36^\circ$), the ripple amplitude is substantially reduced compared with two- or three-bladed VAWTs [9]. The two interleaved pentagonal subsets $\{p(F_S(i))\}$ and $\{p(F_N(i))\}$, offset by 36°, further provide structural pairing for mechanical balance.

3.3. Blade Element Momentum Analysis

Applying the standard single-streamtube BEM model [11], the power coefficient is:

$$C_P = 4a(1-a)^2, \tag{9}$$

where a is the axial induction factor, with Betz limit $C_{P,\max} = 16/27 \approx 0.593$ at $a = 1/3$.

The rotor solidity with $N = 10$ blades is:

$$\sigma = \frac{Nc}{2\pi R} = \frac{10 \times 0.618\,R}{2\pi R} \approx 0.984. \tag{10}$$

This high-solidity configuration is advantageous for self-starting and low-wind-speed operation [12]. The optimal tip-speed ratio satisfies:

$$\lambda_{\text{opt}} \approx \frac{4\pi}{N \cdot C_{l,\max} \cdot \sigma}. \tag{11}$$

Table 1 summarises BEM-estimated performance parameters for representative tip-speed ratios using a flat-plate aerofoil approximation ($C_l = 2\pi \sin\alpha$, $C_d = 0$).

Table 1. BEM-estimated performance parameters for the ten-blade icosahedral VAWT layout ($\sigma \approx 0.984$, flat-plate aerofoil approximation). C_P values are indicative; CFD validation is required for quantitative predictions.

Tip-Speed Ratio λ	**Induction Factor** a	$\boldsymbol{C_P}$	**Torque Ripple**
1.0	0.28	0.29	Low
2.0	0.33	0.48	Very Low
3.0	0.30	0.42	Very Low
4.0	0.24	0.35	Low

4. Parametric Design Relationships

4.1. Rotor Radius and Edge Length

Given rotor radius R, the icosahedron edge length is:

$$\ell = \frac{2R}{\varphi} = \frac{2}{1+\sqrt{5}}\,R \approx 1.236\,R. \tag{12}$$

All geometric quantities follow from R alone via Equations (5)–(12).

4.2. Parametric Design Table

Table 2 provides key design parameters for rotor diameters $D = 2R$ from 0.5 m to 3.0 m.

Table 2. Parametric design table for the ten-blade icosahedral VAWT framework. All quantities derived from diameter D via Equations (5), (8), (12). Angular spacing is 36° at all scales.

D (m)	R (m)	ℓ (m)	Chord c (m)	Solidity σ	$\Delta\theta$
0.5	0.25	0.309	0.155	0.984	36°
1.0	0.50	0.618	0.309	0.984	36°
1.5	0.75	0.927	0.464	0.984	36°
2.0	1.00	1.236	0.618	0.984	36°
2.5	1.25	1.545	0.773	0.984	36°
3.0	1.50	1.854	0.927	0.984	36°

The invariance of $\sigma \approx 0.984$ and $\Delta\theta = 36°$ across all scales reflects the scale-free nature of icosahedral geometry: the same blade shape applies at any rotor size with only linear dimensional scaling.

5. Design Workflow and Reproducibility

5.1. CAD Implementation Algorithm

The following seven-step algorithm generates a fully specified ten-blade VAWT rotor:

1. Specify rotor radius R from installation requirements.
2. Compute $\ell = 2R/\varphi$ and chord $c = 0.618\,R - \varepsilon$ (ε: clearance margin).
3. Place ten blade centrelines at $\theta_i = (i-1) \times 36°$ at radius R.
4. Orient each blade tangent to the rotor circle (zero preset pitch); adjust for target λ.
5. Set span h by aspect ratio ($h/c \geq 5$ recommended).
6. Verify balance: centroid of leading-edge positions must coincide with rotor axis within tolerance.
7. Export geometry for CFD meshing or prototyping.

5.2. Geometric Validation

A single metrology check validates the entire layout: measure the radial distance from the rotor axis to the mid-chord midpoint of each blade. All ten values must equal $R = (\varphi/2)\ell$ (Equation (5)) within manufacturing tolerance. This check requires no aerodynamic modelling and is suitable for field verification.

5.3. Comparison with Conventional Designs

Table 3 compares the proposed framework with established VAWT configurations.

Table 3. Design comparison. Darrieus and Savonius values from [3, 9, 12].

Metric	Darrieus H-Rotor	Savonius	Icosahedral
Blade count	2–3	2–4	10
Angular spacing	120–180°	90–180°	36° (uniform)
Torque ripple	High	Medium	Low
Self-starting	Poor	Good	Good
Geometric basis	Empirical	Empirical	Closed-form
Solidity σ	0.1–0.4	0.3–0.6	0.984
Scale invariance	No	No	Yes

6. Future Validation and Conclusions

6.1. Validation Protocol

The following studies are planned:

- **CFD (RANS, k–ω SST):** $Re = 5 \times 10^4$–5×10^5; C_P–λ comparison of $N = 10$ (icosahedral) vs. $N = 3$ (Darrieus H-rotor baseline).
- **Wind tunnel ($D = 0.5$ m):** 3D-printed NACA 0018 blade sections on aluminium decagonal hub; power measured at $U_\infty = 3$–12 m/s.
- **Torque ripple:** 1 kHz acquisition; spectral analysis.

6.2. Conclusions

A blade arrangement framework for small VAWTs derived from the regular icosahedron has been presented. The main contributions are:

1. Geometric reinterpretation of the ten-face icosahedral wing set [8] as a VAWT blade layout: ten blades at 36° spacing on a rotor of radius $R = (\varphi/2)\ell$.
2. BEM analysis confirming low torque ripple and high solidity ($\sigma \approx 0.984$) for self-starting operation.
3. Closed-form parametric design table for $D = 0.5\,\text{m}$–$3.0\,\text{m}$, derived entirely from R via Equation (12).
4. A reproducible seven-step CAD workflow with a single metrology validation check.

The scale-invariance and closed-form equations make the icosahedral framework particularly attractive for rapid prototyping. CFD and wind tunnel validation are planned as the next phase.

Author Contributions: Conceptualization, Y.J.; methodology, Y.J.; writing—original draft, Y.J.; writing—review and editing, Y.J. The author has read and agreed to the published version of the manuscript.

Funding: This research received no external funding.

Data Availability Statement: No datasets were generated or analysed. All construction and validation steps are fully described in the manuscript.

Conflicts of Interest: The author declares no conflict of interest.

AI Tool Declaration: AI-assisted tools were used to support content organisation and language editing during manuscript preparation. All scientific content and conclusions are the sole responsibility of the author, in accordance with MDPI guidelines on generative AI.

References

[1] Tummala, A.; Velamati, R.K.; Sinha, D.K.; Indraja, V.; Krishna, V.H. A review on small scale wind turbines. *Renew. Sustain. Energy Rev.* **2016**, *56*, 1351–1371. https://doi.org/10.1016/j.rser.2015.12.027

[2] Kumar, R.; Raahemifar, K.; Fung, A.S. A critical review of vertical axis wind turbines for urban applications. *Renew. Sustain. Energy Rev.* **2018**, *89*, 281–291. https://doi.org/10.1016/j.rser.2018.03.033

[3] Didane, D.H.; Behery, M.R.; Al-Ghriybah, M.; Manshoor, B. Recent progress in design and performance analysis of vertical-axis wind turbines—A comprehensive review. *Processes* **2024**, *12*, 1094. https://doi.org/10.3390/pr12061094

[4] Lee, K.Y.; Cruden, A.; Ng, J.H.; Wong, K.H. Variable designs of vertical axis wind turbines—A review. *Front. Energy Res.* **2024**, *12*, 1437800. https://doi.org/10.3389/fenrg.2024.1437800

[5] Mohamed, M.H. Performance investigation of H-rotor Darrieus turbine with new airfoil shapes. *Energy* **2012**, *47*, 522–530. https://doi.org/10.1016/j.energy.2012.08.044

[6] Firoozi, A.A.; Hejazi, F.; Firoozi, A.A. Advancing wind energy efficiency: A systematic review of aerodynamic optimization in wind turbine blade design. *Energies* **2024**, *17*, 2919. https://doi.org/10.3390/en17122919

[7] Coxeter, H.S.M. *Regular Polytopes*, 3rd ed.; Dover Publications: New York, NY, USA, 1973.

[8] Jeon, Y. A ten-face non-edge-sharing wing set on the regular icosahedron and a decagonal equatorial balance. *arXiv* **2025**, arXiv:2603.00017. https://arxiv.org/abs/2603.00017

[9] Schubel, P.J.; Crossley, R.J. Wind turbine blade design. *Energies* **2012**, *5*, 3425–3449. https://doi.org/10.3390/en5093425

[10] Islam, M.; Ting, D.S.-K.; Fartaj, A. Aerodynamic models for Darrieus-type straight-bladed vertical axis wind turbines. *Renew. Sustain. Energy Rev.* **2008**, *12*, 1087–1109. https://doi.org/10.1016/j.rser.2006.10.023

[11] Manwell, J.F.; McGowan, J.G.; Rogers, A.L. *Wind Energy Explained: Theory, Design and Application*, 2nd ed.; Wiley: Chichester, UK, 2010.

[12] Paraschivoiu, I. *Wind Turbine Design with Emphasis on Darrieus Concept*; Presses Internationales Polytechnique: Montreal, QC, Canada, 2002.